Cell, Vol. 113, 469–482, May 16, 2003, Copyright ©2003 by Cell Press

The Pathogen-Inducible Nitric Oxide Synthase (iNOS) in Plants Is a Variant of the P Protein of the Glycine Decarboxylase Complex

Meena R. Chandok,[1] A. Jimmy Ytterberg,[2] Klaas J. van Wijk,[2] and Daniel F. Klessig[1,*]
[1]Boyce Thompson Institute for Plant Research
[2]Department of Plant Biology
Cornell University
Tower Road
Ithaca, New York 14853

Summary

A growing body of evidence indicates that nitric oxide (NO) plays important signaling roles in plants. However, the enzyme(s) responsible for its synthesis after infection was unknown. Here, we demonstrate that the pathogen-induced, NO-synthesizing enzyme is a variant form of the P protein of glycine decarboxylase (GDC). Inhibitors of the P protein of GDC block its NO synthase (NOS)-like activity, and variant P produced in *E. coli* or insect cells displays NOS activity. The plant enzyme shares many biochemical and kinetic properties with animal NOSs. However, only a few of the critical motifs associated with NO production in animals can be recognized in the variant P sequence, suggesting that it uses very different chemistry for NO synthesis. Since nitrate reductase is likely responsible for NO production in uninfected or nonelicited plants, our results suggest that plants, like animals, use multiple enzymes for the synthesis of this critical hormone.

Introduction

A number of signaling molecules or hormones have been implicated in regulating plant defense reactions to pathogens, including salicylic acid (SA), jasmonates, and ethylene (for review see Dong, 2001; Dempsey et al., 1999). In addition, a growing body of evidence suggests that nitric oxide (NO) plays a role in activating resistance responses (for review see Van Camp et al., 1998; Durner and Klessig, 1999; McDowell and Dangl, 2000; Beligni and Lamattina, 2001; Wendehenne et al., 2001). For example, exogenously supplied NO induces defense gene expression and/or production of antimicrobial compounds known as phytoalexins in various plant species (Delledonne et al., 1998, 2001; Durner et al., 1998; Klessig et al., 2000; Noritake et al., 1996; Modolo et al., 2002). NO also potentiates pathogen- and reactive oxygen species (ROS)-induced cell death in soybean suspension cells and tobacco, and NO synthase (NOS) inhibitors block the hypersensitive resistance response (HR) in *Arabidopsis* (Delledonne et al., 1998, 2001). In addition, a burst of NO was detected within minutes of treating tobacco with an oomycete elicitor (Foissner et al., 2000). Since this increase coincided with a burst of ROS, it is possible that NO and ROS work together to signal plant defense responses through a mechanism analogous to that used in animals (for review see Mayer and Hemmens, 1997; Van Camp et al., 1998; McDowell and Dangl, 2000). Beyond defense signaling, NO has been implicated in regulating multiple plant processes, including photomorphogenesis, root growth, leaf expansion, senescence, stomatal closure, and the cytokinin signaling pathway (Mata and Lamattina, 2002; Neill et al., 2002; Tun et al., 2001; for review see Beligni and Lamattina, 2001). Together these data argue that NO serves as an important second messenger in plants, as well as animals (Brunori et al., 1999; Chung et al., 2001).

In animals, NO is produced during the conversion of L-arginine (Arg) to citrulline by a family of enzymes termed NOS (for review see Nathan and Xie, 1994; Alderton et al., 2001). The active form of these enzymes is a homodimer, but since two monomers of calmodulin (CaM) are required for activity, the holoenzyme is actually a heterotetramer. Animal NOSs also contain several tightly-bound cofactors, including heme, FAD, FMN, and tetrahydrobiopterin (H_4B), and they catalyze the conversion of Arg, NADPH, and O_2 to NO, citrulline, and $NADP^+$. In mammals, three distinct isoforms of NOS have been identified; they represent the products of three different genes, with 51%–57% homology between the human isoforms. nNOS is the predominant form in *n*euronal tissue, whereas iNOS is the isoform associated with *i*mmune and inflammatory responses; it is *i*nduced in a wide range of cells and tissues. eNOS is the isoform first found in vascular *e*ndothelial tissue.

While NOS activity has been described in diverse organisms ranging from bacteria to animals (for review see Torreilles, 2001), a plant NOS with obvious homology to the mammalian enzymes has yet to be isolated. However, NOS-like activities have been detected in several plant species (Durner et al., 1998; Foissner et al., 2000; Delledonne et al., 1998; Modolo et al., 2002; Tun et al., 2001; Barroso et al., 1999; Ribeiro et al., 1999; Cueto et al., 1996; Mackerness et al., 2001). Interestingly, NO production in nonelicited sunflower and spinach leaves appears to be mediated by nitrate reductase (NR; Rockel et al., 2002). NR-mediated NO generation also may play a role in abscisic acid-induced stomatal closure in *Arabidopsis* (Desikan et al., 2002), and earlier studies demonstrated that plant NRs can convert nitrite to NO under certain conditions in vitro (for review see Yamasaki et al., 1999; Kaiser et al., 2002). However, there is no evidence that NR plays a role in pathogen infection. Thus, two different enzymes may be responsible for NO production in plants, with an NOS-like enzyme generating NO after pathogen infection and NR producing NO in non-elicited plants. Such "division of labor" in NO production would somewhat parallel the situation in mammals, where the three NOS isoforms play roles in different physiological processes such as relaxation of vascular muscle tissue (eNOS), neurotransmission (nNOS), or regulation of the immune and inflammatory responses (iNOS). Consistent with this possibility, we demonstrate in this paper that the major pathogen-induced NO synthesizing enzyme is not NR but, rather, a variant form

*Correspondence: dfk8@cornell.edu

of the P protein of the glycine decarboxylase complex (GDC).

Results

TMV Inoculation Induces an NOS-like Activity in a Resistance-Specific Manner

Previously, NOS activity was investigated in TMV-resistant (Xanthi nc [NN]) and TMV-susceptible (Xanthi [nn]) tobacco that had been shifted from 32°C to 22°C at 48 hr post infection (hpi; Durner et al., 1998). Since *N* gene-mediated resistance to TMV is temperature sensitive, Xanthi nc (NN) plants maintained at 32°C fail to accumulate SA, express *PR* genes, develop necrotic lesions (HR), or restrict viral replication and spread (Malamy et al., 1992). Upon shifting to permissive temperatures, these responses are strongly activated in a rapid and nearly synchronous manner. NOS-like activity also was found to increase ~5 fold within 3 hr of the temperature shift in TMV-inoculated Xanthi nc (NN), but not Xanthi nn, plants. This NOS-like activity required the cofactors NADPH, FAD, and FMN, and was inhibited by the animal NOS inhibitors L-N^G-monomethyl-L-arginine monoacetate and (L-NMMA) and diphenyleneiodonium chloride. However, while pathogen infection consistently stimulated this NOS-like enzyme, the actual level of NOS activity was highly variable.

To improve detection of the tobacco NOS-like enzyme, the extraction conditions were modified (see Experimental Procedures). In addition, NOS activity was measured using an oxy-hemoglobin assay, which monitors the NO-mediated conversion of the oxygenated, ferrous form of hemoglobin (HbO_2) to ferric methemoglobin (metHb), as well as by the citrulline assay. Using the optimized extraction and assay conditions, the induction of NOS activity in TMV-infected, temperature-shifted Xanthi nc (NN) tobacco was found to be more rapid and substantially greater than previously detected (Figure 1A). An approximately 9-fold increase was detected by 1 hr post shift (hps); NOS activity then increased another ~2 fold to peak at 4 hps before decreasing gradually out to 8 hps. By contrast, no increase in NOS activity was detected in mock-inoculated Xanthi nc (NN) or TMV-inoculated Xanthi (nn) plants following the temperature shift (Figure 1A). NOS activity also was monitored in pathogen-inoculated Xanthi nc (NN) plants maintained at 22°C. In response to TMV inoculation, a 5-fold increase in NOS activity was detected by 2 hr post inoculation (hpi), and a 25- to 30-fold increase was observed by 22 hpi (Figure 1B). Similarly, a large (7 fold), although transient, increase in NOS activity was exhibited by Xanthi nc (NN) plants inoculated with the nonhost pathogen *Pseudomonas syringae* pv. *maculicola*, which induces a variety of defense responses including HR formation (data not shown). In all of these studies, NOS activity depended on the substrate Arg and the cofactors CaM, NADPH, FAD, and H_4B. Thus, activation of defense responses in tobacco resisting infection by avirulent or nonhost pathogens is associated with increased NOS-like activity.

Purification of the Tobacco NOS-like Activity

Although NOS-like activities have been detected in a wide variety of plants, previous efforts to purify a plant NOS or clone its encoding gene were unsuccessful. Indeed, analysis of the complete *Arabidopsis* genome failed to detect an NOS-like gene. Thus, while the tobacco NOS-like activity exhibited similar cofactor requirements and inhibitor sensitivities as mammalian NOSs, it remained unclear whether this enzyme was an NOS. To establish its identity, we developed a purification scheme that involved G-25 Sephadex column chromatography, ammonium sulfate precipitation, and four additional column chromatography steps (see Experimental Procedures for details). This purification scheme is summarized in Table 1 (top), and typical elution profiles for total protein concentration and NOS-like activity from the final four chromatography steps are shown in Figure 2. Following fractionation of the 0%–35% ammonium sulfate precipitate on DEAE-Sepharose, a single, broad peak of NOS activity was detected (Figure 2A). The fractions containing peak NOS activity were pooled and sequentially subjected to ARG-Sepharose (Figure 2B), ADP-Sepharose (Figure 2C), and CaM-Sepharose (Figure 2D) chromatography. In all of these chromatographic steps, only a single major peak of NOS activity was detected by the oxy-hemoglobin assay in the presence of Arg as the substrate. SDS-PAGE analysis of the pooled fractions from each purification step revealed the presence of four major bands in the peak NOS-containing fractions eluted from the CaM-Sepharose column. These included a doublet of approximately 120 kDa and 115 kDa and two lower molecular weight (MW) bands of 50 kDa and 35–37 kDa (Figure 1C). Through this purification scheme, the NOS-like activity was purified ~33,000-fold from approximately 8 kg of TMV-infected tobacco leaves (Table 1, top). The purified protein exhibited a specific activity of 984 nmol min^{-1} mg^{-1} and represented approximately 0.000005%–0.000015% of the total soluble protein or approximately 50–150 pg/mg protein.

To ensure that we were purifying an NOS-like enzyme, rather than nitrate reductase or another enzyme capable of generating NO (Rockel et al., 2002), the oxy-hemoglobin assays were performed in parallel using either Arg or N-hydroxy-L-arginine (NOHA) as the substrate. NOHA is the intermediate formed during the conversion of Arg to NO and citrulline by all eukaryotic NOSs; it is not a substrate for NR. Similar levels of NOS activity were detected when either substrate was provided (Figure 2). NOS activity also was monitored using a citrulline assay, which is the standard assay used in animal systems. Comparable levels of NOS activity were detected in the crude extract and fractions from the different purification steps by the citrulline and oxy-hemoglobin assays (Figure 3A). Finally, the purified tobacco enzyme was shown to have NOS activity using another standard NOS assay, the Greiss assay (data not shown). Taken together, these results argue that the tobacco protein is an NOS-like enzyme.

Characterization of the Putative Tobacco NOS

Characterization of animal NOSs has revealed that they are sensitive to various inhibitors and require several cofactors, including CaM, NADPH, FAD, and FMN. To further establish that the purified tobacco enzyme is NOS like, we monitored its sensitivity to two widely used

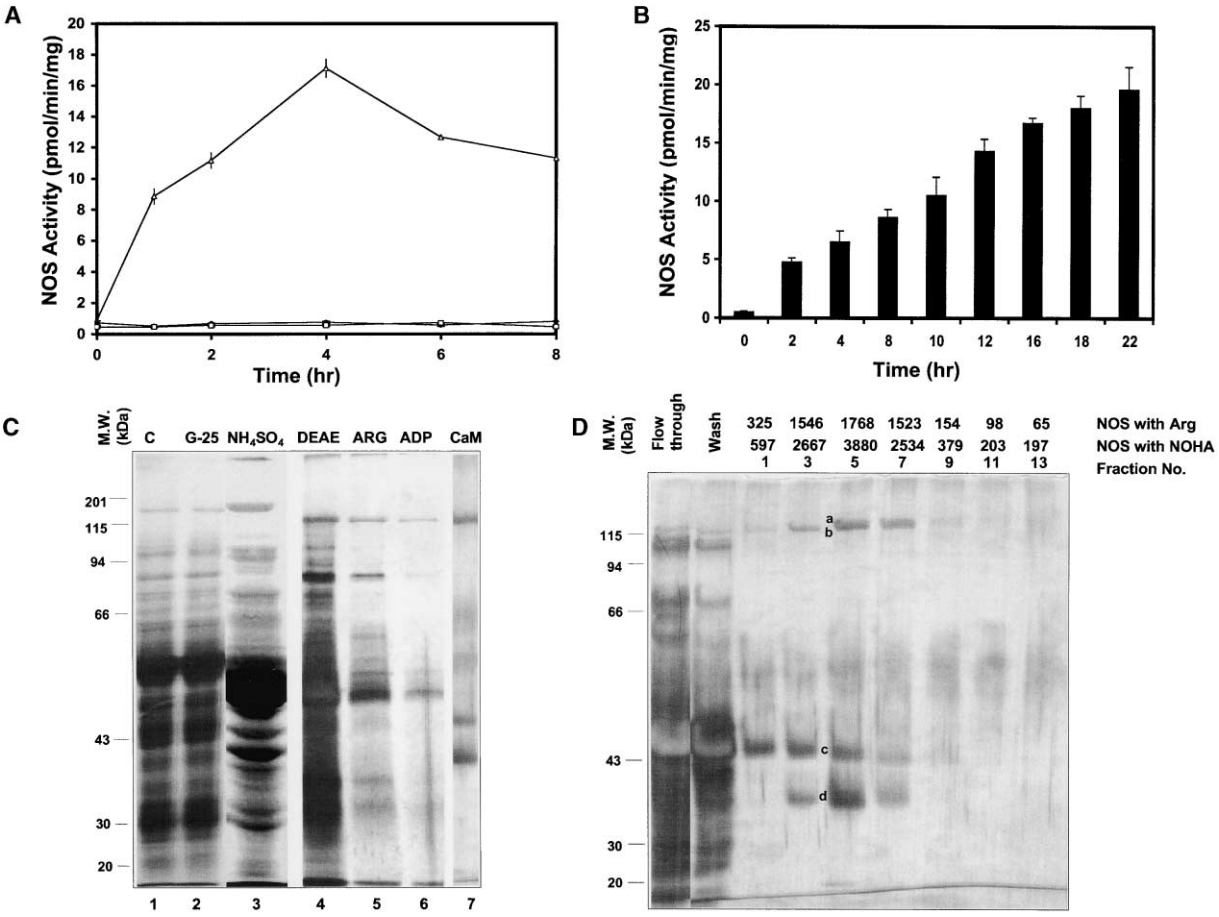

Figure 1. Resistance-Specific Induction of NOS-like Activity by TMV and Protein Profiles from the Purification of the Tobacco NOS-like Activity

(A) NOS activity in leaf extracts of mock or TMV-infected tobacco leaves following a temperature shift. Xanthi nc (NN) plants were infected with TMV (Δ) or mock inoculated with buffer (□), and Xanthi (nn) plants were infected with TMV (■). The plants were inoculated and maintained at 32°C for 48 hpi, then shifted to 22°C to rapidly activate defense responses. The time plotted on the *x* axis is in hr post shift to 22°C. NOS activity was measured at 401 nm using the oxy-hemoglobin assay. The data represent the mean of three independent experiments, with each time point in each experiment determined by assaying NOS activity in triplicate. Thus, the data in each time point represents the average of nine assays. Standard errors are indicated.

(B) NOS activity in extracts of leaves from TMV-inoculated Xanthi nc (NN) plants maintained at 22°C. Extracts were prepared from samples harvested at the designated times post infection. As above, NOS activity was measured at 401 nm using the oxy-hemoglobin assay, and the data represent the mean of three independent experiments. Standard errors are indicated.

(C) SDS-PAGE analysis of fractions from each step of the NOS purification protocol. Aliquots from fractions containing peak NOS-like activity after each purification step were subjected to SDS-PAGE analysis (10%). The proteins in lanes 2–4 were visualized with Coomassie blue; those in lanes 5–8 were detected by silver staining. Lanes 1–7 are from the same gel, while lane 8 was taken from a separate gel shown in (D) (fraction 5). The sizes of the molecular weight (MW) markers are noted in kDa at the left of the gel. Abbreviations: M, MW markers; C, crude; G-25, G-25 Sephadex; $(NH_4)_2SO_4$, ammonium sulfate fraction; DEAE, DEAE-Sepharose; ARG, ARG-Sepharose; ADP, ADP-Sepharose; CaM, CaM-Sepharose.

(D) Protein profiles and NOS-like activity of CaM-Sepharose column fractions. The proteins in fraction numbers 1–13 from the CaM-Sepharose column were subjected to SDS-PAGE (10%) and visualized by silver staining. The positions of the MW size marker (in kDa) are designated on the left of the gel. NOS-like activity, which was assayed using the oxy-hemoglobin assay with either Arg or NOHA as the substrate, is shown above each fraction in pmol/min/25 μl. The four major bands labeled a–d in fraction 5, which contained peak NOS-like activity, were identified by nano-ESI-MS/MS (a and b, which cannot be distinguished on the reproduction of the silver-stained gel, were excised separately; a corresponds to a variant P subunit of glycine decarboxylase [GDC] while b is glutamate synthase [GltS]. c is the large subunit of ribulose bisphosphophosphate carboxylase and d is plastidic aldolase).

inhibitors of animal NOSs, L-NMMA and aminoguanidine. Both inhibitors suppressed the NOS activity of the purified protein in a concentration-dependent manner (Figure 3B), although L-NMMA inhibited it to a greater extent than aminoguanidine. To determine if this L-NMMA-sensitive NOS is the major source of NO production in TMV-infected tobacco, we monitored NO levels in vivo using diaminofluorescein diacetate (DAF-2DA). In mock (data not shown) or uninfected tobacco leaves (Figure 3Cb), little NO is present to convert DAF-2DA to the fluorescent triazole derivative DAF-2T. The intense fluorescence at 26 hr after TMV infection indicates an abundant level of NO (Figure 3Cd) and is consistent with the dramatic rise in NOS-like activity shown in Figure 1B. Addition of L-NMMA at 20 hpi resulted in a dramatic reduction of fluorescence at 26 hpi (Figure 3Cf), arguing

Table 1. Purification and Characterization of the Putative Tobacco NOS

Purification of the Inducible Tobacco NOS-like Activity

Fraction	Protein (mg)	Total Activity (nmol/min)	Specific Activity (nmol/min/mg)	Fold	Recovery (%)
Crude	16,000	480.0	0.03	1	100
$(NH_4)_2SO_4$	842	320.0	0.38	13	66.6
DEAE-Sepharose	49	291.5	6.0	198	60.7
ARG-Sepharose	1.9	89.1	46.9	1,564	18.6
ADP-Sepharose	0.8	63.5	79.4	2,646	13.2
CaM-Sepharose	0.02	19.7	983.7	32,790	4.1

Comparison of the Putative Tobacco NOS with Animal NOSs

Properties	Animal NOSs	Putative Tobacco NOS
Size	130–160 kDa	115–120 kDa
Dependency on H_4B, FAD, NADPH, and O_2	+	+
Ca^{2+} requirement	+	+
CaM requirement	+	+
Inhibition by L-NMMA	+	+
Inhibition by aminoguanidine	+	+
Change in flavin fluorescence with CaM	+	+
Change in tryptophan fluorescence with CaM	+	+
NO synthesis detected by citrulline formation assay	+	+
NO synthesis detected by oxy-hemoglobin assay with either Arg or NOHA as substrate	+	+
NO synthesis detected by Greiss assay	+	+

Comparison of Kinetic Parameters of Plant iNOSs to Animal iNOSs

Kinetic Constants	Tobacco[a]	Arabidopsis[a]	Animal iNOSs	Reference
Specific activity	~20 μmol/min/mg	~47 μmol/min/mg	0.7–1.3 μmol/min/mg	Stuehr, 1996 Stuehr et al., 1991
Km Arginine	7.46 μM	9.79 μM	2.3–19 μM (mammalian) 11–12 μM (fish)	Griffith and Stuehr, 1995 Barroso et al., 2000
Km NADPH	383.14 nM	400 nM	300 nM (mouse) 300 nM (human macrophage)	Griffith and Stuehr, 1995 Stuehr and Griffith, 1992
EC50 calcium	2.79 nM	3.73 nM	N/A[b] (guinea pig hepatocytes)	Geller et al., 1993
EC50 CaM	8.90 nM	7.13 nM	N/A[b] (guinea pig hepatocytes)	Shirato et al., 1998
EC50 FAD	343.40 nM	322.40 nM	200 nM (human macrophages)	Stuehr and Griffith, 1992
EC50 H_4B	734.18 nM	956.75 nM	30 nM (human macrophages)	Stuehr and Griffith, 1992
Ki L-NMMA	6.67 μM	7.58 μM	3.9 μM (rat macrophages)	Reif and McCreedy, 1995

[a] Determined by citrulline assay for enzymes purified from TMV-infected tobacco leaves or from *E. coli* expressing the recombinant Arabidopsis *varP* gene.

[b] Most animal iNOS do not require exogenous additions of calcium or CaM and therefore EC50 for them are not applicable (N/A); however, guinea pig hepatocytes contain an iNOS whose activity is suppressed by CaM inhibitors.

that the purified L-NMMA-sensitive NOS-like enzyme is responsible for the majority of NO production in tobacco leaves resisting TMV infection.

Whether the tobacco NOS-like enzyme required CaM also was investigated. For animal NOSs, CaM binding stimulates NO synthesis by enhancing electron transfer from NADPH to the flavins, and subsequently to the heme. This CaM-stimulated activation of the reductase domain can be detected as a change in the emission spectra of tryptophan and flavin. Similar to animal NOSs, the purified tobacco NOS-like enzyme exhibited elevated tryptophan (Figure 3D) and flavin (Figure 3E) fluorescence in the presence of increasing concentrations of CaM. Furthermore, this phenomenon was suppressed by increasing concentrations of EDTA, which chelates Ca^{2+} and thereby causes CaM to dissociate from NOS. A summary of the biochemical properties of the putative tobacco NOS is presented in Table 1 (middle).

The Tobacco NOS-like Protein Is a Variant P Protein of Glycine Decarboxylase

To determine the identity of the bands detected by SDS-PAGE following CaM-Sepharose chromatography (Figures 1C and 1D), tryptic peptides were generated by in gel digestion and sequenced by manual nano-electrospray tandem mass spectroscopy (ESI-MS/MS). Database searches of the molecular ions against NCBI indicated that the ~120 kDa band (band a in Figure 1D) matched the *Arabidopsis* homologs of the P protein of glycine decarboxylase (GDC), the ~115 kDa protein was the tobacco ferredoxin-dependent glutamate synthase (Fd-GltS) (band b), and the lower, well-resolved bands were the tobacco large subunit (LSU) of ribulose bisphosphate carboxylase (RuBPCase; band c) and tobacco plastidic aldolase (band d). A careful comparison between NOS activity levels and the band intensities corresponding to these proteins in fractions eluted from

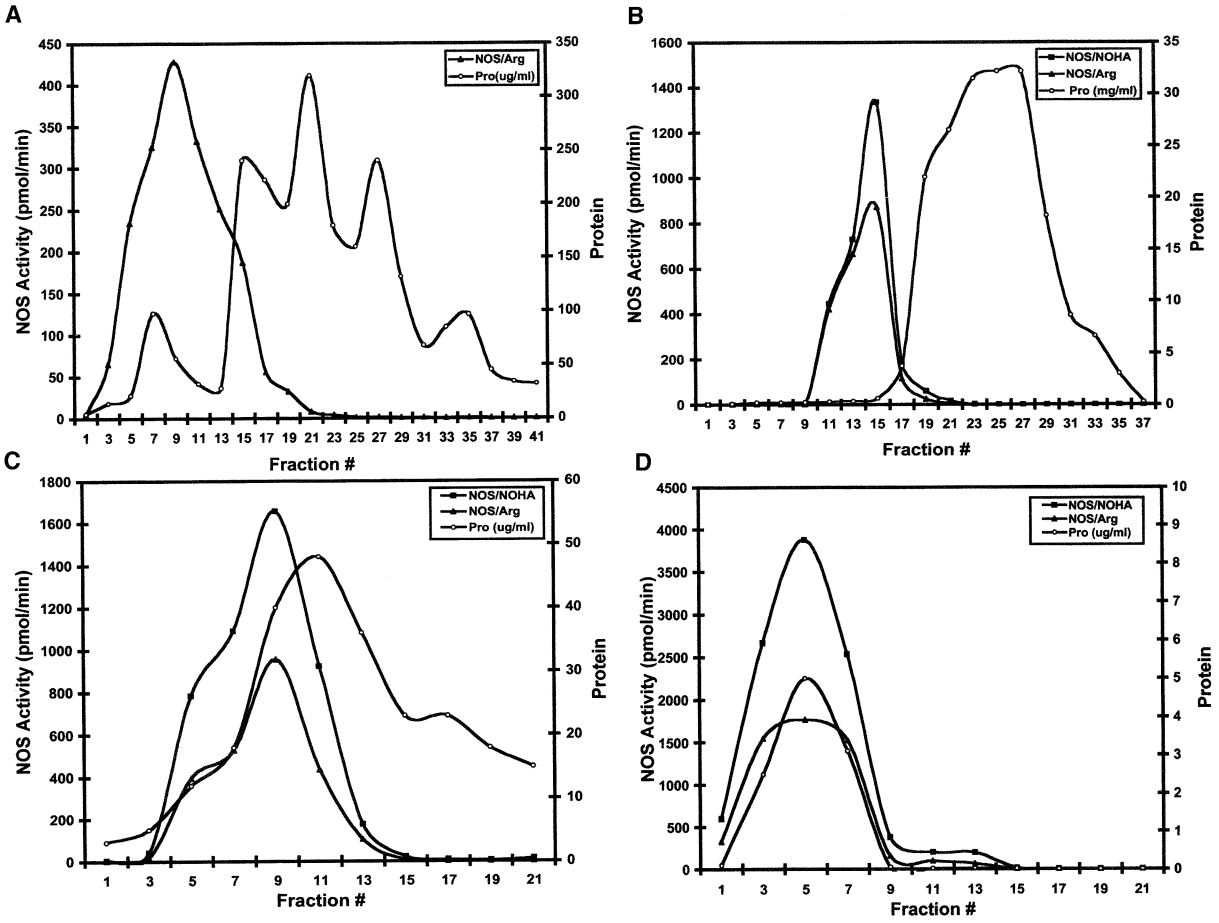

Figure 2. Elution Profiles of NOS-like Activity and Protein Concentration from the Final Chromatography Steps

(A) DEAE-Sepharose column. The void volume fraction from G-25 Sephadex chromatography, which contained most of the NOS-like activity, was subjected to differential ammonium sulfate precipitation. The 0%–35% ammonium sulfate precipitate was dissolved in equilibration buffer and loaded onto a DEAE-Sepharose column. After washing, a linear NaCl gradient (0–0.5 M) was used for protein elution. NOS-like activity was determined in alternate fractions using the oxy-hemoglobin assay with Arg as substrate, and total protein (Pro) content was determined by Bradford analysis.

(B) ARG-Sepharose column. Following DEAE-Sepharose chromatography, fractions containing peak NOS activity (numbers 3–15) were pooled and loaded onto an ARG-Sepharose column. Proteins were eluted with a linear NaCl gradient (0–0.5 M) and alternate fractions were assayed for NOS-like activity using the oxy-hemoglobin assay with NOHA, as well as Arg as substrates, and for total protein content.

(C) ADP-Sepharose column. Fractions containing peak NOS-like activity from ARG-Sepharose chromatography (numbers 9–15) were pooled and loaded onto an ADP-Sepharose column. Protein elution was done with a linear NaCl gradient (0–1.0 M) and determination of NOS-like activity was as described in (B).

(D) CaM-Sepharose column. Fractions containing peak NOS-like activity from ADP-Sepharose chromatography (numbers 3–9) were pooled and loaded onto a CaM-Sepharose column. A linear gradient of EGTA (0–1.0 mM) was used for protein elution and alternate fractions were assayed for NOS-like activity using Arg or NOHA as substrates.

CaM-Sepharose chromatography suggested that the P protein of GDC and/or Fd-GltS is the tobacco NOS-like activity (Figure 1D). MS analysis performed on other preparations of highly purified tobacco NOS-like activity also suggested that the P protein of GDC copurified with NOS activity.

Analysis of the *Arabidopsis* genome identified two genes that might encode the P protein of GDC (*At4g33010* and *At2g26080*). Allowing for minor aa substitutions, the deduced sequences of both genes matched four peptides assembled by manually annotating the MS/MS spectra. Since *At4g33010* required less substitution to match the tobacco sequence, we designated it *varP*, for the variant P protein that is a candidate for NO synthesizing activity; its deduced aa sequence is shown in Figure 4A.

The GDCs form a unique class of amino acid decarboxylases for which there is little direct structural information (Sandmeier et al., 1994). However, sequence analysis of variant P identified several motifs that are similar in function to those found in mammalian NOSs (Figures 4B and 4C). The homology of the putative flavin binding site of variant P with the isoalloxazine motif of mammalian NOSs and other FAD-requiring enzymes is limited (Figure 4C). However, the observations that the tobacco enzyme requires FAD (Table 1, middle) and has a flavin emission spectra (Figure 3D) argue that this motif or a yet-to-be-identified motif participates in flavin

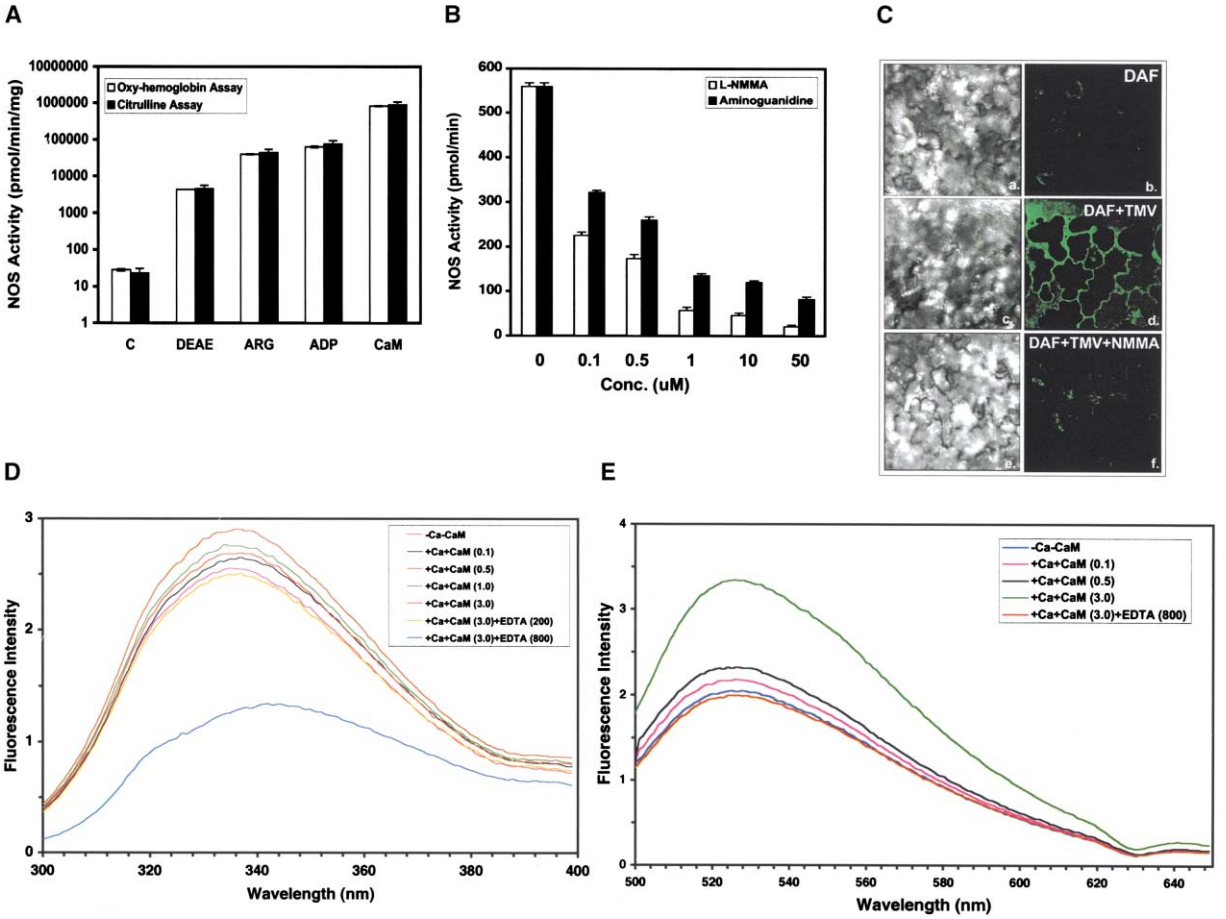

Figure 3. Characterization of the Putative Tobacco NOS

(A) The oxy-hemoglobin and citrulline assays detect similar levels of tobacco NOS-like activity. NOS activity was measured in the crude extract and in pooled peak fractions from each step of the purification protocol using the oxy-hemoglobin and citrulline assays. The data shown are the average of three independent experiments. Abbreviations: C, crude; DEAE, DEAE-Sepharose; ADP, ADP-Sepharose; ARG, ARG-Sepharose; CaM, CaM-Sepharose. Standard errors are indicated.

(B) Tobacco NOS-like activity is suppressed by animal NOS inhibitors. The effect of increasing concentrations of the NOS inhibitors L-NMMA and aminoguanidine on the activity of the purified tobacco NOS-like enzyme was determined using the oxy-hemoglobin assay with Arg as the substrate. Standard errors are indicated.

(C) Confocal microscopy of TMV-induced intracellular DAF-2DA fluorescence. Sections of tobacco Xanthi nc (NN) leaves 24 hpi with TMV were loaded with DAF-2DA, incubated for 2 hr in darkness, washed, and examined by confocal laser microscopy: (a) bright field image of uninfected leaf section loaded with DAF-2DA, (b) fluorescence of DAF-2T (503–530 nm) of the same sample as in (a), (c) bright field image of TMV-infected tissue, (d) fluorescence of DAF-2T (503–530 nm) of the same sample as in (c), (e) bright field image of TMV-infected tissue incubated with inhibitor L-NMMA starting at 20 hpi and DAF-2DA at 24 hpi, and (f) fluorescence of DAF-2T of the same sample as in (e).

(D) Tryptophan fluorescence of the NOS-like protein was monitored in the absence of Ca^{2+} and CaM or in the presence of 100 μM Ca^{2+} and different concentrations of CaM (μM) and EDTA (μM), as indicated in the inset. The protein was irradiated at 288–300 nm and emission spectra were recorded at 300–390 nm.

(E) Flavin fluorescence of the tobacco NOS-like protein was monitored as described in (D), except that the protein was irradiated at 450–460 nm, and the emission spectra were recorded at 500–650 nm.

binding. Both variant P and P (At2g26080) also contain a pyridoxal phosphate (PP) binding domain, which covalently binds this cofactor, and also likely forms an NADPH binding-Rossman fold (Figure 4D). Interestingly, the lysine to which PP likely is covalently attached is surrounded by a combination of histidines and cysteines; they could serve as a 2Fe-2S cluster to coordinate the binding of another cofactor, such as an Fe cluster or heme. Consistent with this possibility, recombinant variant P protein requires heme for NOS activity (see below) and a typical Soret band at 416 nm, which is indicative of heme incorporation, appeared in the absorption spectra of the purified recombinant protein following incubation with heme (data not shown).

At2g26080 encodes a protein, designated P, which is 89% identical to variant P and contains at least two of the above motifs. However, its N-terminal 80 aa are only 63% identical to those of variant P, and the sequences flanking the putative flavin binding site, which might participate in Arg binding, show only limited homology with variant P. Thus, it seems unlikely that P has NOS activity. The subcellular localization predictors TargetP (http://www.cbs.dtu.dk/services/TargetP/) and Predotar (http://www.inra.fr/Internet/Produits/Predotar/) suggest that both variant P and P are targeted to the mitochondria by predicted N-terminal transit peptides of 39 and 41 aa, respectively. However, since various motifs required for NO synthesis and CaM binding are located

A

```
MERARRLAYRGIVKRLVNDTKRHRNAETPHLVPHAPARYVSSLSPFISTPRSVNHTAAFGRHQQTRSISVDAVKPSDTFP  80
RRHNSATPDEQTHMAKFCGFDHIDSLIDATVPKSIRLDSMKFSKFDAGLTESQMIQHMVDLASKNKVFKSFIGMGYYNTH 160
VPTVILRNIMENPAWYTQYTPYQAEISQGRLESLLNFQTVITDLTGLPMSNASLLDEGTAAAEAMAMCNNILKGKKKTFV 240
IASNCHPQTIDVCKTRADGFDLKVVTSDLKDIDYSSGDVCGVLVQYPGTEGEVLDYAEFVKNAHANGVKVVMATDLLAL 320
TVLKPPGEFGADIVVGSAQRFGVPMGYGGPHAAFLATSQEYKRMMPGRIIGISVDSSGKQALRMAMQTREQHIRRDKATS 400
NICTAQALLANMAAMYAVYHGPAGLKSIAQRVHGLAGIFSLGLNKLGVAEVQELPFFDTVKIKCSDAHAIADAASKSEIN 480
LRVVDSTTITASFDETTTLDDVDKLFKVFASGKPVPFTAESLAPEVQNSIPSSLTRESPYLTHPIFNMYHTEHELLRYIHKL 560
QSKDLSLCHSMIPLGSCTMKLNATTEMMPVTWPSFTDIHPFAPVEQAQGYQEMFENLGDLLCTITGFDSFSLQPNAGAA 640
GEYAGLMVIRAYHMSRGDHHRNVCIIPVSAHGTNPASAAMCGMKIITVGTDAKGNINIEEVRKAAEANKDNLAALMVTY 720
PSTHGVYEEGIDEICNIIHENGGQVYMDGANMNAQVGLTSPGFIGADVCHLNLHKTFCIPHGGGGPGMGPIGVKNHLAPFL 800
PSHPVIPTGGIPQPEKTAPLGAISAAPWGSALILPISYTYIAMMGSGGLTDASKIAILNANYMAKRLEKHYPVLFRGVNGTV 880
AREFIIDLRGFKNTAGIEPEDVAKRLMDYGFHGPTMSWPVPGTLMIEPTESESKAELDRFCDALISIREEIAQIEKGNADVQN 960
NVLKGAPHPPSLLMADTWKKPYSREYAAFPAPWLRSSKFWPTTGRVDNVYGDRKLVCTLLPEEEQVAAAVSA          1037
```

B

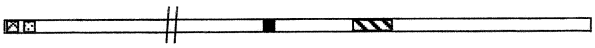

- Putative CaM binding site (8-28 aa)
- Putative flavin binding site (34-44 aa), alignment shown in **C**
- Leucine zipper, possibly for dimerization (575-596 aa)
- Pyridoxal phosphate binding domain/ putative NADPH binding-Rossmann fold (746-813 aa), alignment shown in **D**

C

Isoalloxazine motif for flavin binding

```
HA--PARYVSSLS  Arb VarP
TTVTPSRYVSSVS  Arb P
--KKLRLYSIASS  Pea FNR
--LQARYYSIASS  Rat CPR
--LQPRYYSISSS  Rat NOS
--LTPRLYSIAS A E.coli SR
```

D **PLP peptide segment of the pyridoxal phosphate binding domain**

```
                                                  *
NGGQVYMDGANMNAQVGLTSPGFIGADVCHLNLHKTFCIP  Arb VarP
NGGQVYMDGANMNAQVGLTSPGFIGADVCHLNLHKTFCIP  Arb P
NGGQVYMDGANMNAQVGLTSPGWIGADVCHLNLHKTFCIP  Pea
HGGQVYLDGANMNAGVGLCRPGDYGSDVSHLNLHKTFCIP  Chicken

HGGGGPGMGPIGVK  Arb VarP
HGGGGPGMGPIGVK  Arb P
HGGGGPGMGPIGVK  Pea
HGGGGPGMGPIGVK  Chicken
```

Figure 4. The Predicted Amino Acid Sequence and Structural Motifs of the Variant P Protein

(A) The deduced aa sequence of the *Arabidopsis* variant P protein (At4g33010); the underlined sequences correspond to the four peptides (but two have substitutions) derived from the putative tobacco NOS-like activity that were sequenced by ESI-MS/MS. Substitutions were observed in GNINIEEIR (I replaced by V in *Arabidopsis*) and in FGVPHGYGGPHAAFLATSQEYKR (M replaced the first H). Note that the mass spectrometer cannot distinguish between isobars (e.g., I and L).

(B) Schematic representation of several putative cofactor binding sites in the variant P protein, which may participate in NO synthesis.

(C) Sequence comparison of the putative flavin binding site (isoalloxazine motif) of the variant P and P proteins of *Arabidopsis* with those of a mammalian NOS and other FAD-requiring enzymes.

(D) Sequence comparison of the active site polypeptide (PLP) from the P protein of chicken liver GDC (Fujiwara et al., 1987) with the deduced aa sequences of variant P and P from *Arabidopsis* and P from pea. The lys to which PP is likely attached is indicated by an asterisk. Cys and His residues, which might serve as a 2Fe-2S cluster to coordinate binding of another cofactor in the plant enzymes, are boxed.

partly or entirely within the predicted transit sequence, either variant P is not localized to the mitochondria or, if it is targeted there, the transit sequence is not removed. Targeting of the mitochondrial transcription factor Mtf1 to this organelle without cleavage of the transit sequence (Biswas and Getz, 2002) provides precedence for the latter possibility. A third alternative is that the *Arabidopsis* sequence was misannotated and the real translational start site is further upstream. This common mistake could result in a protein whose N terminus does not contain a mitochondrial transit sequence or has a transit sequence upstream of the annotated N terminus (Peltier et al., 2002).

The Variant P Protein of GDC Exhibits NOS Activity

To assess whether variant P has NOS activity, we tested whether the P protein inhibitors carboxymethoxylamine (CM) and aminoacetonitrile (Douce et al., 2001; Yao et al., 2002) suppressed the ability of the tobacco enzyme to synthesize NO. In the presence of NADPH and either NOHA or Arg as the substrate, the highly purified tobacco enzyme exhibited high levels of NOS activity,

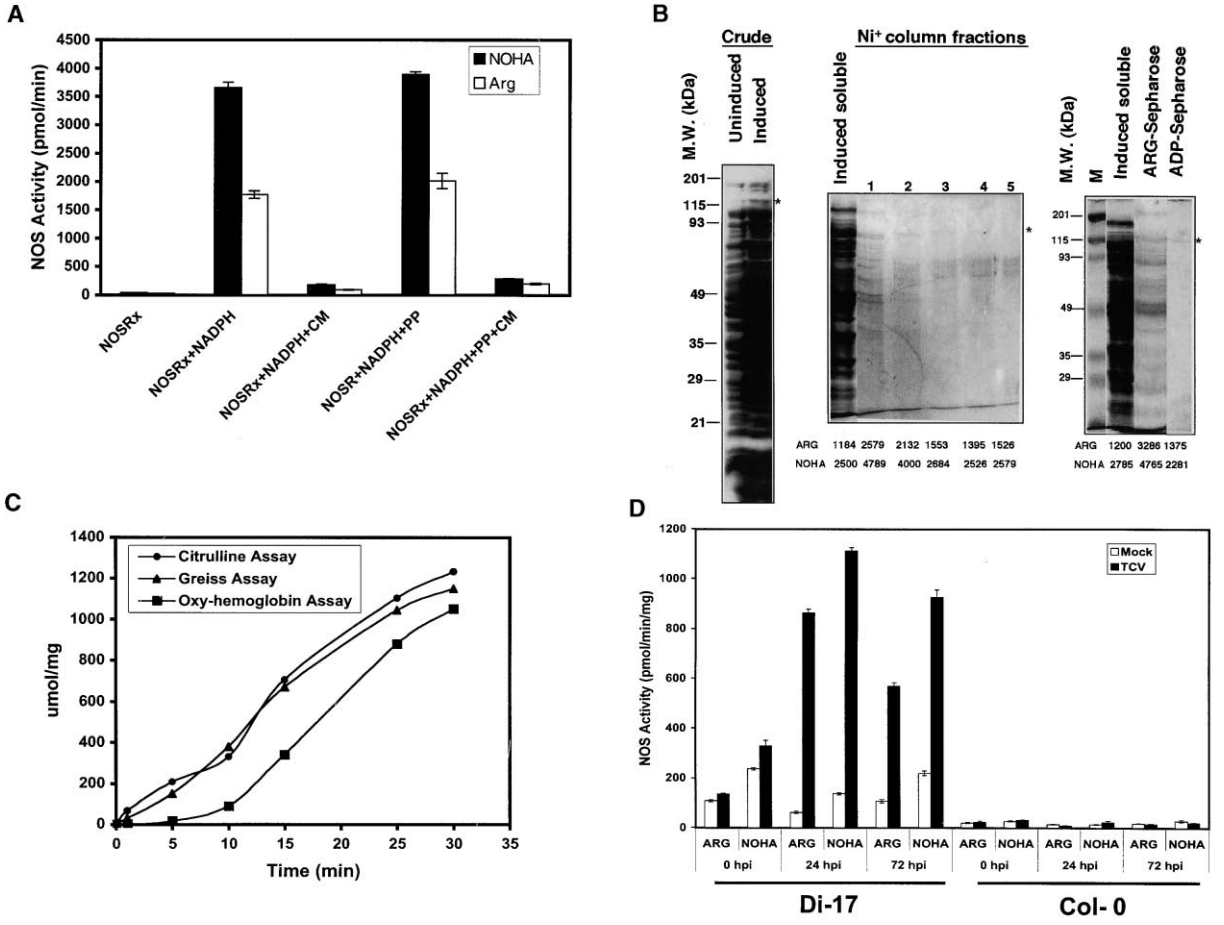

Figure 5. The Variant P Protein of GDC Is the Plant iNOS

(A) An inhibitor of P proteins blocks the tobacco NOS-like activity. The effect of the P protein inhibitor carboxymethoxylamine (CM; 200 μM) on the tobacco NOS-like activity was monitored using the oxy-hemoglobin assay and either Arg or NOHA as the substrate. In addition to the highly purified tobacco NOS-like enzyme, all NOS assay reactions (NOSRx) contained a complete set of cofactors except NADPH, which was added where indicated. The effect of pyridoxal phosphate (PP) on NOS activity was also assessed.

(B) Recombinant his_6-tagged variant P protein exhibits NOS activity. The left shows SDS-PAGE analysis (10%) of crude *E. coli* extracts that either lack (uninduced) or express *varP* (induced). NOS activity, as determined by the oxy-hemoglobin assay using Arg or NOHA as the substrate, is expressed below each lane in pmol/mg/min. The asterisk marks the position of recombinant variant P protein, and the position of MW markers is noted in kDa at the left of the gel. A soluble fraction from *E. coli* expressing *varP* also was subjected to SDS-PAGE analysis (10%) following Ni^+ affinity chromatography (center) or sequential affinity chromatography on ARG-Sepharose and ADP-Sepharose (right). The crude extract shown on the left corresponds to Expt. #1 in Table 2, and the Ni^+ affinity purified fractions correspond to Expt. #2.

(C) Time course of NO and citrulline formation by the recombinant *Arabidopsis varP*-encoded protein using Arg as substrate. The purified recombinant protein made in *E. coli* after heme addition was used as starting material. Reactions were carried out at 37°C in presence of 1 mM Arg (or 1 mM nitro-L-arginine), 1 mM magnesium diacetate, 1 mM $CaCl_2$, 1 μM CaM, and 4 μM FAD (see Experimental Procedures). The reaction was started by addition of NADPH to 100 μM and H_4B to 10 μM for the oxy-hemoglobin assay. For the Greiss and citrulline assays, the reaction was started by addition of the enzyme to reaction mixtures containing NADPH and H_4B. Production of labeled citrulline from ^{14}C-labeled Arg was monitored as described by Bredt and Snyder (1989). In the Greiss assay, the NOS reaction was stopped by heat inactivation at 50°C for 10 min or by addition of 200 mM EDTA, and nitrate was converted back to nitrite by incubation with NR for 30 min at 37°C before addition of the Greiss reagent to determine (indirectly) the level of NO production.

(D) iNOS is activated in *Arabidopsis* resisting TCV infection. NOS-like activity was monitored in mock- and TCV-inoculated Di-17 (resistant) and Col-0 (susceptible) *Arabidopsis* plants at 0, 24, and 72 hpi using the oxy-hemoglobin assay with either Arg or NOHA as the substrate.

which were inhibited approximately 90%–95% by addition of 200 μM CM (Figure 5A). Similar results were observed using a relatively crude extract obtained prior to affinity chromatography (data not shown) or when the highly purified tobacco enzyme was incubated with aminoacetonitrile (data not shown). Thus, inhibitors that block P protein activity suppress the tobacco NOS-like activity. Furthermore, since CM inhibits P protein function by reacting with PP, this result suggests that PP participates in NO synthesis. This is consistent with the observation that addition of PP modestly stimulates the activity of the tobacco enzyme (Figure 5A), perhaps by binding to a small portion of the purified enzyme that did not contain bound PP.

Confirmation that variant P has NOS activity was obtained by expressing His_6-tagged *varP* in *E. coli* and insect Sf9 cells. In crude *E. coli* extracts, induction of *varP* expression corresponded with the accumulation

Table 2. NO Synthesizing Activity of the *Arabidopsis varP*-Encoded Protein Produced in *E. coli* or Baculovirus-Infected Sf9 Cells and Its Dependence on Cofactors H_4B and Heme

	$+H_4B$ +Heme[a]		$+H_4B$ −Heme		$-H_4B$ −Heme	
	ARG	NOHA	ARG	NOHA	ARG	NOHA
E. coli Expt. #1						
Uninduced	44[b]	44	44	44	26	44
Induced	1982	2720	746	965	158	255
E. coli Expt. #2						
Uninduced	70	114	18	70	26	158
Induced[c]	1184	2500	509	1298	158	307
Ni column fractions[d]						
1	2579	4789	1132	2421	53	237
2	2132	4000	921	1711	316	26
3	1553	2684	737	1105	79	737
4	1395	2526	500	921	211	395
5	1526	2579	395	737	132	342
Sf9 cells[e]						
Mock	53	123	18	114	26	61
Empty vector	0	26	0	9	0	70
varP	456	833	272	684	96	219

[a] Arg or NOHA were used as substrate in the presence (+) or absence (−) of the critical cofactors H_4B and Heme as indicated.
[b] NO synthesizing activity was determined with an oxy-hemoglobin assay and is expressed in pmol/min/mg.
[c] Expression of *varP* was induced with 1 mM IPTG and crude total extracts were prepared 6hr later.
[d] The His_6-tagged recombinant variant P from the soluble fraction extracted from the IPTG-induced *E.coli* of Expt. #2 was purified on a Ni^+ column.
[e] Sf9 insect cells were mock infected or infected either with recombinant baculovirus not carrying *varP* (empty vector) or carrying it (*varP*). Extracts were prepared at 72 hpi.

of an ~120 kDa protein and a 45- to 62-fold increase in NOS activity (Figure 5B). Purifying the His_6-tagged variant P by affinity chromatography on a Ni^+ column also enriched an ~120 kDa protein. Moreover, these fractions exhibited 17- to 109-fold greater levels of NOS activity than uninduced cells. Both the purified NOS activity eluted from the Ni^+ column and that detected in the crude extract were dependent on the presence of H_4B and heme (Table 2). A similar enrichment of an ~120 kDa protein and increase in NOS activity was observed when a soluble extract from induced *E. coli* cells was subjected to sequential affinity chromatography with ARG-Sepharose and ADP-Sepharose (Figure 5B). Consistent with these results, insect Sf9 cells infected with recombinant baculovirus expressing His_6-tagged *varP* exhibited 7- to 32-fold greater levels of NOS activity in the presence of H_4B and heme than mock- or empty baculovirus vector-infected cells (Table 2). These results conclusively demonstrate that the variant P protein has NOS activity.

To assess the kinetic properties of the variant P protein, the rate of citrulline and NO formation were measured over time using the citrulline, oxy-hemoglobin, and Greiss assays. All three assays indicated similar kinetics of citrulline and NO synthesis (Figure 5C). Comparable Km's for Arg and Vmax's for the variant P protein were also obtained with the citrulline and Greiss assays (Km = 9.79 μM, Vmax = 40.16 μmol/min/mg with citrulline assay and Km = 10.52 μM, Vmax = 41.66 μmol/min/mg with Greiss assay). Together, these data indicate that both reaction products are made in near equimolar quantities. Additional kinetic parameters of the purified tobacco enzyme and the recombinant *Arabidopsis* enzyme synthesized in *E. coli* were determined using the citrulline assay; they are compared to those of animal iNOSs in Table 1 (bottom).

An NOS-like Activity Is Induced in TCV-Infected *Arabidopsis* in a Resistance-Specific Manner

Our initial analyses indicated that an NOS-like activity is rapidly activated in tobacco resisting pathogen infection. To extend this finding, we monitored NOS activity in *Arabidopsis* plants inoculated with turnip crinkle virus (TCV). By 24 hpi, NOS activity in Di-17 plants, which are resistant to TCV infection, increased 8- to 14-fold over that detected in mock-inoculated control plants (Figure 5D). In comparison, no increase in NOS activity was detected in TCV-susceptible Col-0 plants throughout the time course. Taken together, these results demonstrate that *Arabidopsis*, like tobacco, contains a pathogen-inducible NOS activity, which will be referred to as iNOS.

Discussion

In this paper, we report the first purification and detailed characterization, to our knowledge, of a pathogen-induced NO-synthesizing activity from plants. Following a six-step purification protocol, biochemical and molecular analyses revealed that this plant iNOS is a variant P protein of the GDC complex. Since the variant P protein shares very little sequence homology with animal NOSs, this unexpected discovery explains why previous efforts to identify this enzyme failed.

Plant iNOS versus Animal NOSs

Despite the lack of sequence homology, the biochemical properties of the plant enzyme, including cofactor requirements and inhibitor sensitivity, as well as its kinetic properties (with the exception of H_4B; Table 1, bottom), appear to be very similar to those of its animal counterparts (Table 1, middle). Moreover, plant iNOS, like that

of animals, is specifically induced during the resistance response to pathogen infection (Figures 1A and 5D).

A critical similarity between plant and animal iNOSs is that their activation is required to signal defense responses following pathogen attack. In plants, NOS inhibitors block pathogen- or elicitor-induced defense gene activation (Delledonne et al., 1998; Durner et al., 1998; Klessig et al., 2000), synthesis of antimicrobial compounds (Modolo et al., 2002), and HR formation (Delledonne et al., 1998, 2001). Similarly, these inhibitors worsen the course of disease caused by diverse pathogens in animals (for review see MacMicking et al., 1997; Nathan and Shiloh, 2000; Bogdan, 2001). Moreover, mice containing knockout mutations in both copies of the iNOS gene are more susceptible than wild-type mice to pathogen infection (for review see Bogdan, 2001). Comparable experiments are under way to assess the role of the plant iNOS in disease resistance.

In mammals, NOS activity is highly controlled, as might be anticipated, since its product is a potent regulator of many physiological processes. Despite more than a decade of intense study, the extent and sophistication of NOS regulation has become evident only in the past several years (for review see Alderton et al., 2001; Bogdan, 2001). The mammalian iNOS is regulated primarily at the transcriptional level (for review see Alderton et al., 2001). Consistent with this finding, preliminary studies indicate a dramatic rise in *varP* mRNA levels in TCV-infected resistant Di-17, but not in susceptible Col-0 (data not shown). However, the rapid elevation of NO within 3–6 min after treatment of tobacco leaf epidermal cells with the defense elicitor cryptogein (Foissner et al., 2000) suggests that iNOS is also regulated at the posttranslational level. Since both Ca^{2+} and CaM are required for the plant iNOS activity, it is possible that this rapid activation is mediated by CaM and changes in Ca^{2+} levels, as is the case for mammalian eNOS and nNOS. Alternatively, the rapid increase in NOS activity following infection or elicitor treatment might be due to stimulation of a distinct, constitutively expressed NOS-like enzyme. Supporting this latter possibility, immunoblot analyses with antibodies raised against animal NOSs have identified constitutively expressed proteins of 166 kDa in maize (Ribeiro et al., 1999) and soybean (Modolo et al., 2002), and 130 kDa in pea (Barroso et al., 1999). Caution must be exercised when interpreting these data, however, since we have detected considerable cross reactivity between tobacco proteins and similar antibodies prepared against mammalian NOSs. This cross reactivity may be due to the presence of cofactor binding motifs found in animal NOSs and unrelated plant proteins that may not have NO synthesizing capacity.

In contrast to the sizes of the soybean, maize, and pea proteins recognized by antibodies raised against animal NOSs, the purified tobacco iNOS and recombinant *Arabidopsis* variant P protein appear to be ~120 kDa. This size is consistent with a deduced molecular mass of 113 kDa for the *Arabidopsis* protein. Taken together, our study and earlier reports suggest that there are at least two, and possibly three, enzymes responsible for NO synthesis in plants: nitrate reductase, which is associated with nonelicited NO generation (Desikan et al., 2002; Kaiser et al., 2002; Rockel et al., 2002); iNOS, which is responsible for the dramatic and sustained NO production in plants resisting pathogens (this report); and perhaps a constitutive NOS that is rapidly (and possibly transiently) activated by pathogens or pathogen-derived elicitors (Foissner et al., 2000; Modolo et al., 2002). Therefore, plants may employ as much division of labor for NO synthesis as mammals.

The plant iNOS, like its mammalian counterpart, is present in vanishingly low amounts in uninfected plants. Even after a 33,000-fold purification from TMV-infected leaves, which exhibit a 20-to 30-fold increase in NOS activity, the tobacco iNOS represented 5% or less of the protein in the purest fraction (Figure 1D). Assuming 5%, the specific activity of the purified iNOS would be ~20 μmol/min/mg (Table 1, top); this activity is similar to the ~47 μmol/min/mg for the purified *Arabidopsis* variant P synthesized in *E. coli* (data not shown). Note this is approximately 15- to 30-fold higher than that of purified mammalian iNOS (Stuehr et al., 1991; Stuehr, 1996). Interestingly, the amount of NOS activity in crude extracts prepared from *Arabidopsis* resisting TCV infection (863 pmol/min/mg; Figure 5C) was approximately 30- to 45-fold higher than that detected in tobacco resisting infection by TMV (19–30 pmol/min/mg; Figure 1 and Table 1, top) or by *P. syringae* pv. *maculicola* (19 pmol/min/mg). At present, the reason(s) for this large difference is unclear. Perhaps tobacco extracts contain an inhibitor that suppresses iNOS activity. Alternatively, different plant species might contain different levels of NOS activity. Supporting this possibility, an activated mouse macrophage cell line contained over 10-fold more iNOS activity than an induced human adenocarcinoma cell line (Stuehr et al., 1991; Garvey et al., 1996).

The GDC Complex and Plant Variant P/iNOS

The GDC multienzyme complex, which is over 1300 kDa in size, is present in the mitochondrial matrix of plant and animal cells and is also found in microbes (for review see Douce et al., 2001). In addition to the 100–120 kDa pyridoxal phosphate-containing P protein, the GDC complex contains L protein, a 50–60 kDa lipoamide dehydrogenase; T protein, a 40–45 kDa tetrahydrofolate-containing enzyme; and H protein, an ~15 kDa lipoamide-containing enzyme. This complex, along with serine hydroxymethyltransferase, catalyzes the conversion of two glycine molecules into serine, CO_2, and NH_3. In green plant tissue, the GDC subunits represent up to 50% of the mitochondrial protein; this massive amount of enzyme is used to salvage glycine produced by RuBP-Case (a key photosynthetic enzyme) during photorespiration.

The N-terminal ~80 aa of P proteins, which include the predicted transit sequence, differ markedly between plants and their animal and microbial counterparts. Interestingly, most of aa differences between the P protein, which presumably forms part of GDC, and the variant P (iNOS) of *Arabidopsis* also reside in this region. Despite 89% identity and 92% similarity overall, these proteins contain 30 aa differences in their N-terminal 80 aa. Some of this variation may reflect the generally lower level of homology observed in transit sequences as compared with the mature protein sequences of orthologous nuclear-encoded organellar proteins (Peltier et al.,

2002). Nonetheless, 20 of these 30 differences are C-terminal to the predicted transit sequence. Since two putative binding sites for factors required for NOS activity (CaM and flavin) are in the N-terminal 80 aa of the variant P protein, animal and microbial P proteins associated with the GDC complex are unlikely to have NOS activity. At present we do not know if the *Arabidopsis* P protein encoded by *At2g26080* has NOS activity. However, we suspect it does not but, rather, is part of the GDC complex. As such, it would be present in very large amounts in the mitochondria of green tissue, including leaves. If P were to have NOS activity, leaves would be expected to contain very high levels of this activity even in the absence of infection; this was not detected in tobacco or *Arabidopsis*. By contrast, the extremely low level of NOS-like activity detected even in tobacco resisting TMV infection suggests that the variant P genes of tobacco and *Arabidopsis* are expressed at extremely low levels and/or only under certain conditions, such as during a disease resistance response.

In contrast to GDC, which is targeted to the mitochondria, the subcellular location of variant P/iNOS is currently unclear. The rapid appearance of NO within the chloroplasts of tobacco epidermal cells after treatment with an oomycete elicitor (Foissner et al., 2000) suggests that iNOS is located in this organelle. (Alternatively, a constitutive, chloroplastic NOS might be responsible for this extremely rapid production of NO, rather than iNOS.) Regardless, the variant P/iNOS does not appear to be part of the GDC complex, since the GDC and NOS-like activities (iNOS) do not copurify (data not shown) and tobacco iNOS has an estimated native molecular mass of 280 kDa as determined by gel filtration on Sephacryl S-300 (data not shown), while that of the GDC complex is at least 350 kDa in vitro and may approach >1300 kDa in vivo. Based on its estimated native molecular mass, iNOS likely functions as a dimer; this would be consistent with the presence of a leucine zipper in its sequence (Figure 4B).

P Proteins and Disease

There is precedence for the involvement of the P protein (or a variant form of it) in both plant and animal pathology. In ducks, a variant form of P serves as the coreceptor for the duck Hepatitis B virus (Li et al., 1999). In oats, the P protein of susceptible, but not resistant, cultivars binds the fungal toxin victorin in vivo (Wolpert et al., 1994; Navarre and Wolpert, 1995). Victorin, which is produced by the fungus *Cochliobolus victoriae* (the causal agent of victoria blight disease) also is a potent inhibitor of GDC activity in vivo (Navarre and Wolpert, 1995). Thus, it was proposed that victorin exerts its host genotype-specific toxicity via inhibition of GDC activity.

Victorin also induces a variety of host-selective, defense-type responses, including host cell death, that mirror those induced by race-specific elicitors (Navarre and Wolpert, 1999). A dominant allele of the *Vb* gene was shown to confer susceptibility to *C. victoriae* and its toxin. Interestingly, *Vb* is genetically inseparable from *Pc-2*, a gene that confers resistance to the crown rust pathogen *Puccinia coronata* (Wolpert et al., 1994). One possible explanation for this result is that *Vb* and *Pc-2* are the same gene and that they encode a modified form of variant P whose NOS activity or responsiveness to infection or a pathogen-derived ligand (such as victorin) is altered, perhaps enhanced. Since NO appears to participate in pathogen-induced programmed host cell death (for review see Wendehenne et al., 2001), perhaps elevated NO production by the *Vb*/*Pc-2*-encoded variant P might stimulate an HR and resistance to the biotrophic *P. coronata*. By contrast, increased NO synthesis following *C. victoriae* infection might enhance susceptibility by increasing the availability of nutrients from dying host cells, thereby enhancing growth during the necrotrophic phase of this hemibiotrophic pathogen.

In summary, our results demonstrate that plants, like animals, contain an iNOS that is activated in a resistance-specific manner following pathogen infection. The surprising discovery that plant iNOS is a variant P protein of the GDC complex explains the many difficulties encountered during attempts to isolate this enzyme. Moreover, identification of the plant iNOS will open novel avenues for understanding both how NO mediates disease resistance in plants and the chemistry of NO synthesis.

Experimental Procedures

Plant Material and Viral Infection

Tobacco plants (Nicotiana cv. Xanthi nc [NN] or Xanthi [nn]) were grown as described before (Conrath et al., 1995). TMV infection was done using either 4- to 6-week-old plants or excised leaves. Tissue was infected with TMV (1 μg/ml in 10 mM Hepes buffer [pH. 7.0] in the presence of carborundum). Mock inoculation was performed using buffer with carborundum. Following inoculation, cut leaves were floated on buffer soaked Whatman 3MM paper in plastic trays covered with plastic wrap and kept at 22°C in a growth chamber programmed on a 14 hr light, 10 hr dark cycle. Samples were taken at the indicated times and frozen in liquid nitrogen prior to NOS activity and protein determination. For temperature shift experiments, plants were moved to 32°C 40 hr before infection, and defense responses were activated by shifting plants from 32°C to 22°C at 48 hpi.

Arabidopsis Di-17 and Col-0 plants were grown as described before (Shah et al., 1999). Viral infections were performed using transcripts synthesized in vitro from a cloned cDNA of the TCV genome using T7 RNA polymerase (Dempsey et al., 1993). For inoculations, the viral transcript was suspended at a concentration of 2.5 μg/200 μl in inoculation buffer, and the infection was performed as described earlier (Dempsey et al., 1993). Leaves were removed at various times for NOS activity and protein determination.

Purification of the Tobacco NOS-like Protein

The inoculated leaves of TMV-infected tobacco plants maintained at 22°C were harvested at 20–22 hpi and stored at −80°C. A minimum of 8–10 kg of tissue was used to begin the purification protocol. The five-step purification scheme is outlined in Table 1 (top) and the results presented in Figures 1 and 2. For a detailed description of the purification protocol see the Supplemental Experimental Procedures section online at http://www.cell.com/cgi/content/full/113/4/469/DC1.

Fluorescence Spectroscopy

Tryptophan and flavin fluorescence were measured as described by Gachhui et al. (1996), using an SLM 8000 spectrofluorometer. Briefly, the purified NOS eluted from the CaM-Sepharose column was diluted to 2 μg/ml in 10 mM Hepes (pH 7.0) in a 0.5 ml quartz cuvette. Measurements (at 25°C) were initiated by irradiating the protein at 288–300 nm for tryptophan fluorescence and 450–460 nm for flavin fluorescence. The emission spectra were recorded at 300–390 nm for tryptophan and 500–600 nm for flavin, before and after the addition of $CaCl_2$ (100 μM) in presence of different concentrations of CaM (0.1–3.0 μM) to induce the formation of a CaM-

NOS complex. Dissociation of this complex was monitored following addition of EDTA (200 and 800 μM). The mixture was stirred in the cuvette for 5 min after each addition.

NOS Activity Assays

NOS activity was measured using the oxy-hemoglobin assay (Murphy and Noack, 1994) with slight modifications. Briefly, a reaction mixture (total volume of 1 ml) in 10 mM Hepes (pH, 7.0) contained enzyme (200 μl from crude or G-25 Sephadex or 100 μl from the other purification steps), 1 mM Arg or 100 μM NOHA or 1 mM nitro-L-arginine, 1 mM magnesium diacetate, 1 mM $CaCl_2$, 1 μM CaM, and 4 μM FAD; this was incubated at 37°C for 30 min. Reactions were stopped by heat inactivation at 50°C for 10 min or by addition of 200 mM EDTA. To ensure that this assay accurately reflected NOS activity, duplicate reactions were performed in the presence or absence of nitro-L-arginine. Since this arginine analog inhibits NOS activity, any metHb generated in its presence is produced by nonspecific HbO_2 oxidation. NOS activity was determined by subtracting the amount of metHb produced in the presence of this inhibitor from the amount generated in its absence. Therefore, this assay would not detect the NO synthesis activity of NR. The reaction was started by addition of NADPH to 100 μM and H_4B to 10 μM. The change in absorbance was recorded at 401 nm. Citrulline assays were done according to the procedure of Bredt and Snyder (1989). The Greiss assay was done according to Hevel and Marletta (1994). For time kinetics experiments using the citrulline and Greiss assays, the reactions were stopped either by heat inactivation at 50°C for 10 min or by adding 200 mM EDTA. The Greiss assay reaction was continued, after inactivating NOS activity, with addition of NR for 30 min as described by Herel and Marletta (1994) before addition of the Greiss reagent.

In Vivo Detection of NO

Tobacco Xanthi nc (NN) plants (3 weeks old) were mock infected or infected with TMV as described above, and a section of the infected leaf was excised at 20 hpi. Leaf sections were incubated in buffer (10 mM Tris/HCl [pH 7.2]) in the presence or absence of 1 mM L-NMMA in the dark for 4 hr with gentle shaking before addition of DAF-2DA to 10 μM and continued incubation for 2 hr. Excess fluorophore was removed by extensive washing, and imaging was done using a confocal laser scanner (Leica). Sections were excited at 488 nm. DAF-2T emission was recorded using a 505–530 nm band-pass filter, and autofluorescence of chloroplasts was captured with a 585 nm long-pass filter. Microscope, laser, and photo-multiplier settings were held constant during the course of an experiment in order to obtain comparable data. Images were processed and analyzed using the Leica lite software. Due to space restriction, the autofluorescence images and the superimposed autofluorescence and DAF-2T fluorescence images are not shown in Figure 3C.

Protein Estimation and SDS-PAGE Analysis

The protein concentration of different column fractions was determined by Bradford analysis (Bradford, 1976). SDS-PAGE analysis was performed on 10%–12% polyacrylamide gels using Laemmli's protocol (Laemmli, 1970), followed by silver staining to visualize the proteins.

Protein Identification by Mass Spectrometry

Following SDS-PAGE, stained protein bands were excised, washed, reduced, and digested with modified trypsin (Promega) according to Shevchenko et al. (1996). The peptides then were extracted and dissolved in 20 μl of 5% formic acid, followed by desalting and concentration using microcolumns (Gobom et al., 1999; Poros R2; Applied Biosystems). The peptides were eluted directly into nanoelectrospray needles (Protana A/S, Odense, Denmark) with 1 μl of 50% methanol and 1% formic acid (Wilm et al., 1996). The spectra were acquired on an electrospray tandem mass spectrometer (Q-TOF; Micromass, Manchester, UK) and used to search the public databases with the program Mascot (http://www.matrix-science.com/). The sequences were confirmed by manual interpretation using MassLynx and PepSeq (Micromass).

Cloning and Expression of Variant P (*varP*) in pET-28a and pFastBac Plasmids

A full-length cDNA clone of *varP* was obtained from the *Arabidopsis* Biological Resource Center (ABRC) and the complete fragment was amplified using the oligos GGATCCATGGAGCGCGCAAGGAGAC TTGC and GTCGACTCAAGCAGACACTGCAGCTGCGAC, which have BamHI and SalI sites, respectively, using Herculase hotstart DNA polymerase (Stratagene). PCR was performed under the following conditions: 2 min at 92°C, 10 s at 92°C, 30 s at 58°C, 3.5 min at 72°C, and 1 min at 72°C for 30 cycles. The purified amplified fragment was ligated to BamHI and SalI digested pET-28a and pFastBac vectors.

Ligation of the PCR-generated fragment to the pET-28a *E. coli* expression vector (Novagen) introduced an N-terminal hexahistidine leader peptide. Fusion variant P proteins were synthesized in the soluble fraction of *E. coli* strain Bl21(DE3) (Novagen) and affinity purified on Ni-NTA agarose (Novagen) in the presence of 8 mM mercaptoethanol, according to manufacturer's instructions, or by using ARG and ADP affinity chromatography as described above.

The PCR-generated *varP* fragment ligated to pFASTBac was transformed into DH10Bac cells (Invitrogen), and the recombinant bacmid was isolated from white colonies according to manufacturer's instructions. Isolated recombinant DNA was used for transfection of Sf9 insect cells as per manufacturer's instructions.

Acknowledgments

We would like to thank Brian Crane for his expert advice and assistance concerning the chemistry of NOSs, Susanne Rasmussen for initial analysis of the tobacco iNOS, and D'Maris Dempsey for assistance in preparation of the manuscript. We also thank Gary Blissard and Oliver Lung for their generous assistance with the baculovirus expression system, Carl Nathan for suggestions on the manuscript, and Carol Bayles for her help in confocal microscopy. The Park and Triad Foundations are gratefully acknowledged and thanked for supporting this research through a "Plants and Human Health Grant" to the Boyce Thompson Institute for Plant Research. This work was also supported in part by the National Science Foundation grant MCB-0110404.

Received: January 13, 2003
Revised: April 24, 2003
Accepted: April 24, 2003
Published: May 15, 2003

References

Alderton, W.K., Cooper, C.E., and Knowles, R.G. (2001). Nitric oxide synthases: structure, function and inhibition. Biochem. J. *357*, 593–615.

Barroso, J.B., Corpas, F.J., Carreras, A., Sandalio, L.M., Valderrama, R., Palma, J.M., Lupiáñez, J.A., and del Río, L.A. (1999). Localization of nitric oxide synthase in plant peroxisomes. J. Biol. Chem. *274*, 36729–36733.

Barroso, J.B., Carreras, A., Esteban, F.J., Peinado, M.A., Martinez-Lara, E., Valderrama, R.A., Rodrigo, J., and Lupianez, J.A. (2000). Molecular and kinetic characterization and cell type location of inducible nitric oxide synthase in fish. Am. J. Physiol. Regul. Integr. Comp. Physiol. *279*, R650–R656.

Beligni, M.V., and Lamattina, L. (2001). Nitric oxide in plants: the history is just beginning. Plant Cell *24*, 267–278.

Biswas, T.K., and Getz, G.S. (2002). Import of yeast mitochondrial transcription factor (Mtf1p) via a nonconventional pathway. J. Biol. Chem. *277*, 45704–45714.

Bogdan, C. (2001). Nitric oxide and the immune response. Nat. Immunol. *2*, 907–916.

Bradford, M.M. (1976). A rapid and sensitive method for the quantitation of microgram quantities of protein utilizing the principle of protein-dye binding. Anal. Biochem. *72*, 248–254.

Bredt, D.S., and Snyder, S.H. (1989). Nitric oxide mediates glutamate-linked enhancement of cGMP levels in the cerebellum. Proc. Natl. Acad. Sci. USA *86*, 9030–9033.

Brunori, M., Giuffre, A., Sarti, P., Stubauer, G., and Wilson, M.T. (1999). Nitric oxide and cellular respiration. Cell. Mol. Life Sci. *56*, 549–557.

Chung, H.T., Pae, H.O., Choi, B.M., Billiar, T.R., and Kim, Y.M. (2001). Nitric oxide as a bioregulator of apoptosis. Biochem. Biophys. Res. Commun. *282*, 1075–1079.

Conrath, U., Chen, Z., Ricigliano, J.R., and Klessig, D.F. (1995). Two inducers of plant defense responses, 2,6-dichloroisonicotinic acid and salicylic acid, inhibit catalase activity in tobacco. Proc. Natl. Acad. Sci. USA *92*, 7143–7147.

Cueto, M., Hernandez-Perera, O., Martin, R., Bentura, M.L., Rodrigo, J., and Lamas, S. (1996). Presence of nitric oxide synthase activity in roots and nodules of *Lupinus albus*. FEBS Lett. *398*, 159–164.

Delledonne, M., Xia, Y., Dixon, R.A., and Lamb, C. (1998). Nitric oxide signal functions in plant disease resistance. Nature *394*, 585–588.

Delledonne, M., Zeier, J., Marocco, A., and Lamb, C. (2001). Signal interactions between nitric oxide and reactive oxygen intermediates in the plant hypersensitive disease resistance response. Proc. Natl. Acad. Sci. USA *98*, 13454–13459.

Dempsey, D., Shah, J., and Klessig, D.F. (1999). Salicylic acid and disease resistance in plants. Crit. Rev. Plant Sci. *18*, 547–575.

Dempsey, D.A., Wobbe, K.K., and Klessig, D.F. (1993). Resistance and susceptible responses of *Arabidopsis thaliana* to turnip crinkle virus. Phytopathology *83*, 1021–1029.

Desikan, R., Griffiths, R., Hancock, J., and Neill, S. (2002). A new role for an old enzyme: Nitrate reductase-mediated nitric oxide generation is required for abscisic acid-induced stomatal closure in *Arabidopsis thaliana*. Proc. Natl. Acad. Sci. USA *99*, 16314–16318.

Dong, X. (2001). Genetic dissection of systemic acquired resistance. Curr. Opin. Plant Biol. *4*, 309–314.

Douce, R., Bourguignon, J., Neuburger, M., and Rébeillé, F. (2001). The glycine decarboxylase system: a fascinating complex. Trends Plant Sci. *6*, 167–176.

Durner, J., and Klessig, D.F. (1999). Nitric oxide as signal in plants. Curr. Opin. Plant Biol. *2*, 369–374.

Durner, J., Wendehenne, D., and Klessig, D.F. (1998). Defense gene induction in tobacco by nitric oxide, cyclic GMP and cyclic ADP ribose. Proc. Natl. Acad. Sci. USA *95*, 10328–10333.

Foissner, I., Wendehenne, D., Langebartels, C., and Durner, J. (2000). In vivo imaging of an elicitor-induced nitric oxide burst in tobacco. Plant J. *23*, 817–824.

Fujiwara, K., Okamura-Ikeda, K., and Motokawa, Y. (1987). Amino acid sequence of the phosphopyridoxyl peptide from P-protein of the chicken liver glycine cleavage system. Biochem. Biophys. Res. Commun. *149*, 621–627.

Gachhui, R., Presta, A., Bentley, D.F., Abu-Soud, H.M., McArthur, R., Brudvig, G., Ghosh, D.K., and Stuehr, D.J. (1996). Characterization of the reductase domain of rat neuronal nitric oxide synthase generated in the methylotrophic yeast Pichia pastoris. Calmodulin response is complete within the reductase domain itself. J. Biol. Chem. *271*, 20594–20602.

Garvey, E.P., Furfine, E.S., and Sherman, P.A. (1996). Purification and inhibitor screening of human nitric oxide synthase isozymes. Methods Enzymol. *269*, 339–349.

Geller, D.A., Lowenstein, C.J., Shapiro, R.A., Nussler, A.K., Silvio, M., Wang, S.C., Nakayama, D.K., Simmons, R.L., Snyder, S.H., and Billiar, T.R. (1993). Molecular cloning and expression of inducible nitric oxide synthase from human hepatocytes. Proc. Natl. Acad. Sci. USA *90*, 3491–3495.

Gobom, J., Nordhoff, E., Mirgorodskaya, E., Ekman, R., and Roepstorff, P. (1999). Sample purification and preparation technique based on nano-scale reversed-phase columns for the sensitive analysis of complex peptide mixtures by matrix-assisted laser desorption/ionization mass spectrometry. J. Mass Spectrom. *34*, 105–116.

Griffith, O.W., and Stuehr, D.J. (1995). Nitric oxide synthases: properties and catalytic mechanism. Annu. Rev. Physiol. *57*, 707–736.

Hevel, J.M., and Marletta, M.A. (1994). Nitric-oxide synthase assays. Methods Enzymol. *233*, 250–258.

Kaiser, W.M., Weiner, H., Kandlbinder, A., Tsai, C.-B., Rockel, P., Sonoda, M., and Planchet, E. (2002). Modulation of nitrate reductase: some new insights, an unusual case and a potentially important side reaction. J. Exp. Biol. *53*, 875–882.

Klessig, D.F., Durner, J., Zhou, J.M., Kumar, D., Navarre, R., Zhang, S., Shah, J., Wendehenne, D., Trifa, Y., Noad, R., et al. (2000). NO and salicylic acid signaling in plant defense. Proc. Natl. Acad. Sci. USA *97*, 8849–8855.

Laemmli, U.K. (1970). Cleavage of structural proteins during the assembly of the head of the bacteriophage T4. Nature *227*, 680–685.

Li, J., Tong, S., and Wands, J.R. (1999). Identification and expression of glycine decarboxylase (p120) as a duck hepatitis B virus pre-S envelope-binding protein. J. Biol. Chem. *274*, 27658–27665.

Mackerness, S.A.-H., John, C.F., Jordan, B., and Thomas, B. (2001). Early signaling components in ultraviolet-B responses: distinct roles for different reactive oxygen species and nitric oxide. FEBS Lett. *489*, 237–242.

MacMicking, J., Xie, Q.-w., and Nathan, C. (1997). Nitric oxide and macrophage function. Annu. Rev. Immunol. *15*, 323–350.

Malamy, J., Hennig, J., and Klessig, D.F. (1992). Temperature-dependent induction of salicylic acid and its conjugates during the resistance response to tobacco mosaic virus infection. Plant Cell *4*, 359–365.

Mata, C.G., and Lamattina, L. (2002). Nitric oxide and abscisic acid cross talk in guard cells. Plant Physiol. *128*, 790–792.

Mayer, B., and Hemmens, B. (1997). Biosynthesis and action of nitric oxide in mammalian cells. Trends Biochem. Sci. *22*, 477–481.

McDowell, J.J., and Dangl, J.L. (2000). Signal transduction in the plant immune response. Trends Biochem. Sci. *25*, 79–82.

Modolo, L.V., Cunha, F.Q., Braga, M.R., and Salgado, I. (2002). Nitric oxide synthase-mediated phytoalexin accumulation in soybean cotyledons in response to the *Diaporthe phaseolorum* f. sp. *meridionalis* elicitor. Plant Physiol. *130*, 1288–1297.

Murphy, M.E., and Noack, E. (1994). Nitric oxide assay using hemoglobin method. Methods Enzymol. *233*, 240–250.

Nathan, C., and Shiloh, M.U. (2000). Reactive oxygen and nitrogen intermediates in the relationship between mammalian hosts and microbial pathogens. Proc. Natl. Acad. Sci. USA *97*, 8841–8848.

Nathan, C., and Xie, Q.W. (1994). Nitric oxide synthases: roles, tolls, and controls. Cell *78*, 915–918.

Navarre, D.A., and Wolpert, T.J. (1995). Inhibition of the glycine decarboxylase multienzyme complex by the host-selective toxin victorin. Plant Cell *7*, 463–471.

Navarre, D.A., and Wolpert, T.J. (1999). Victorin induction of an apoptotic/senescence-like response in oats. Plant Cell *11*, 237–249.

Neill, S.J., Desikan, R., Clarke, A., and Hancock, J.T. (2002). Nitric oxide is a novel component of abscisic acid signaling in stomatal guard cells. Plant Physiol. *128*, 13–16.

Noritake, T., Kawakita, K., and Doke, N. (1996). Nitric oxide induces phytoalexin accumulation in potato tuber tissue. Plant Cell Physiol. *37*, 113–116.

Peltier, J.B., Emanuelsson, O., Kalume, D.E., Ytterberg, J., Friso, G., Rudella, A., Liberles, D.A., Söderberg, L., Roepstorff, P., von Heijne, G., and van Wijk, K.J. (2002). Central functions of the lumenal and peripheral thylakoid proteome of Arabidopsis determined by experimentation and genome-wide prediction. Plant Cell *14*, 211–236.

Reif, D.W., and McCreedy, S.A. (1995). N-nitro-L-arginine and N-monomethyl-L-arginine exhibit a different pattern of inactivation toward the three nitric oxide synthases. Arch. Biochem. Biophys. *32*, 170–176.

Ribeiro, E.A., Jr., Cunha, F.Q., Tamashiro, W.M., and Martins, I.S. (1999). Growth phase-dependent subcellular localization of nitric oxide synthase in maize cells. FEBS Lett. *445*, 283–286.

Rockel, P., Strube, F., Rockel, A., Wildt, J., and Kaiser, W.M. (2002). Regulation of nitric oxide (NO) production by plant nitrate reductase in vivo and in vitro. J. Exp. Bot. *53*, 103–110.

Sandmeier, E., Hale, T.I., and Christen, P. (1994). Multiple evolutionary origin of pyridoxal-5′-phosphate-dependent amino acid decarboxylases. Eur. J. Biochem. *221*, 997–1002.

Shah, J., Kachroo, P., and Klessig, D.F. (1999). The Arabidopsis *ssi1* mutation restores pathogenesis-related gene expression in *npr1* plants and renders defensin gene expression SA dependent. Plant Cell *11*, 191–206.

Shevchenko, A., Wilm, M., Vorm, O., and Mann, M. (1996). Mass spectrometric sequencing of proteins silver-stained polyacrylamide gels. Anal. Chem. *68*, 850–858.

Shirato, M., Sakamoto, T., Uchidia, Y., Nomura, A., Ishii, Y., Goto, Y., and Hasegawa, S. (1998). Molecular cloning and characterization of Ca2+-dependent inducible nitric oxide synthase from guinea pig lung. Biochem. J. *333*, 795–799.

Stuehr, D.J. (1996). Purification and properties of nitric oxide synthases. Methods Enzymol. *268*, 324–333.

Stuehr, D.J., and Griffith, O.W. (1992). Mammalian nitric oxide synthases. Adv. Enzymol. Relat. Areas Mol. Biol. *65*, 287–346.

Stuehr, D.J., Cho, H.J., Kwon, N.S., Weise, M.F., and Nathan, C.F. (1991). Purification and characterization of the cytokine-induced macrophage nitric oxide synthase: an FAD- and FMN-containing flavoprotein. Proc. Natl. Acad. Sci. USA *88*, 7773–7777.

Torreilles, J. (2001). Nitric oxide: one of the more conserved and widespread signaling molecules. Front. Biosci. *6*, D1161–D1172.

Tun, N.N., Holk, A., and Scherer, G.F.E. (2001). Rapid increase of NO release in plant cell cultures induced by cytokinin. FEBS Lett. *509*, 174–176.

Van Camp, W., Van Montagu, M., and Inzé, D. (1998). H_2O_2 and NO: redox signals in disease resistance. Trends Plant Sci. *3*, 330–334.

Wendehenne, D., Pugin, A., Klessig, D.F., and Durner, J. (2001). Nitric oxide: comparative synthesis and signaling in animal and plant cells. Trends Plant Sci. *6*, 177–183.

Wilm, M., Shevchenko, A., Houthaeve, T., Breit, S., Schweigerer, L., Fotsis, T., and Mann, M. (1996). Femtomole sequencing of proteins from polyacrylamide gels by nano-electrospray mass spectrometry. Nature *379*, 466–469.

Wolpert, T.J., Navarre, D.A., Moore, D.L., and Macko, V. (1994). Identification of the 100kD victorin binding protein from oats. Plant Cell *6*, 1145–1155.

Yamasaki, H., Sakihama, Y., and Takahashi, S. (1999). An alternative pathway for nitric oxide production in plants: new features of an old enzyme. Trends Plant Sci. *4*, 128–129.

Yao, N., Tada, Y., Sakamoto, M., Nakayashiki, H., Park, P., Tosa, Y., and Mayama, S. (2002). Mitochondrial oxidative burst involved in apoptotic response in oats. Plant J. *30*, 567–579.